

Hongyu Chen ^{1,2}, Yu Cheng ^{1,4}, Ying Wang ^{1,2}, Yongcheng Ding ^{1,2}, Chenglong Wang ^{1,2,3}, Xuguang Feng ^{1,5}, Qinya Fan ^{1,2}, Feng Yuan ^{1,2}, Guanghe Fu ^{1,2}, Xinqing Zou ^{1,2,3,*}

¹ School of Geographic and Oceanographic Sciences, Nanjing University, Nanjing 210093, China

² Ministry of Education Key Laboratory for Coast and Island Development, Nanjing University, Nanjing 210093, China

³ Collaborative Innovation Center of South China Sea Studies, Nanjing University, Nanjing 210093, China

⁴ Geological Survey of Jiangsu Province, Nanjing, 210018, China

⁵ Laboratory for Marine Geology, Qingdao National Laboratory for Marine Science and Technology, Qingdao 266061, China

Corresponding author: Xinqing Zou (zouxq@nju.edu.cn)

Key Points:

- Plastic production and flood events jointly affect microplastic distribution in the burial record of the Yangtze Estuary.
- The increase of microplastic abundance and diversity in the estuary is caused by the erosion of upstream and land-based during flood.
- Microplastic abundance corresponds well to historic extreme floods and the hydrological cycle of the Yangtze River (8 a and 22 a).

Abstract

Microplastics are ubiquitously found in the environment; however, our knowledge about their storage and mechanism in the burial record is scarce. We selected a core (CCYY1) in the tidal flat of the Yangtze Estuary and investigated its microplastic pollution and sediment grain size. Both plastic production and sediment grain size were significantly positively correlated with microplastic abundance, revealing that the distribution of microplastics in the core was mutually affected by plastic production and extreme flood events. Moreover, the sedimentary record increased rapidly in microplastic abundance and microplastic diversity during the historic extreme flood. The resuspension of upstream microplastics and erosion of land-based microplastics by heavy rain may be responsible for the increase during flood events. Microplastic abundance had a significant period of 8 a and 22 a, indicating the influence of El Niño-Southern Oscillation and solar activity. This study also proposed microplastics as a proxy index for palaeo-flooding.

Plain Language Summary

Microplastics have become ubiquitous in the environment and sediment is a major sink for microplastics. Therefore, the microplastic pollution history would be documented in the sediment, but the burial record of microplastics is poorly

known in current study. We choose a core in a tidal flat of the Yangtze Estuary to explore how and why microplastics in sedimentary record are distributed. The results exhibited increasing fluctuations of microplastic abundance and polymer types over time. This is basically affected by the exponential growth of plastic production. Surprisingly, we found that the high microplastic abundance is related to coarse sediment grain size, which may indicate the influence of the flood events. We verify this viewpoint by comparing microplastic records and historic extreme floods as well as the hydrological period of the Yangtze River. The microplastics was scoured seriously in land and resuspended in upstream river during flood events, causing a rapid increase of microplastics in the estuary. Our study revealed the relationship between microplastics and flood events in the long term, which is beneficial to understand the geophysical process of microplastics.

1 Introduction

Global plastic production has been consistently growing since the 1950s, reaching 368 million tonnes in 2019 (Plastics Europe, 2020). Rivers act as major pathways for land-based plastics debris to enter the ocean, the final sink of plastics and microplastics, with 91% of land-based plastic waste transported to the ocean via rivers (Lebreton & Andrady, 2019). However, the estimated amount of floating plastic debris on the surface of global oceans (7000 35000 tonnes) is markedly less than riverine plastic outflow (0.057 12.7 million tonnes) (Cózar et al., 2014; Jambeck et al., 2015; Mai et al., 2020), suggesting the fragmentation and deposition of unaccounted plastics. Following fragmentation by physical and chemical processes (Laxague et al., 2018; C. Wang et al., 2021), plastics measuring less than 5 mm were classified as microplastics (Arthur et al., 2009). They have become omnipresent in environmental matrices, including water, sediment, atmosphere, ice, and organisms (Amélineau et al., 2016; Besseling et al., 2017; Ding et al., 2021; Veerasingam et al., 2016). When ingested by an organism, microplastics could pose a potential threat to the organism itself and to human health via the food web (Wright et al., 2013). Several factors affect microplastic penetration into the sediment, such as density, biofilm formation (Lobelle & Michael, 2011), and combination with marine snow or animal excrement (Katija et al., 2017; Long et al., 2015). Meteorologically induced hydrological conditions play an important role in this process: floods, storms, rain, and typhoons can significantly change the sediment distribution and storage of microplastics. Therefore, it is necessary to clarify the fluvial and depositional processes of microplastics entering sediment to better understand the transportation of microplastics into the ocean.

The estuary system represents a transition zone of the river and offshore, and it is regarded as a hot spot area of pollution research (Chapman & Wang, 2001; Sun et al., 2012). The river flow becomes slow when entering the estuary zone, and a large amount of sediments and pollutants carried by the river are deposited in this area (Dai et al., 2018). Therefore, the pollution of the whole basin can be reflected in the estuarine pollution (Ridgway & Shimmield, 2002). Meanwhile,

the estuarine delta is the most densely populated area globally, and the pollution in the estuary zone poses significant threat to the health of the population in the estuarine delta. Previously, the study of estuarine microplastic pollution was focused on the microplastics in the surface water and sediment (Gray et al., 2018; S. Zhao et al., 2015); however, few studies have focused on the burial records of microplastics.

Microplastics in the sedimentary core reflect the microplastic storage and long-term changes in an area. Martin et al. (2020) estimated that approximately 160 tonnes of microplastics were deposited in the mangrove sediment of the Red Sea and Arabian Gulf. In most areas affected by an increase in plastic production, the microplastic abundance generally increases from the bottom to the surface of the core (Brandon et al., 2019; Chen et al., 2020). Moreover, the changes in land use can influence the vertical distribution of microplastics (Dahl et al., 2021). However, the effect of other factors (such as the flood event) on microplastic storage is to be determined. The Yangtze River Delta is the first region to produce and consume plastics in China (Y. Jiang & Jiang, 2013); therefore, the analysis of the core in Yangtze River can provide a complete record of microplastic pollution in China. A better understanding of the vertical distribution, influencing factors, and mechanism of microplastics in the core is helpful in providing new insights into microplastic management.

According to many plastic transport models, the Yangtze River is considered the largest plastic-export waterway globally because of its dense surrounding population (Lebreton et al., 2017; Mai et al., 2020; Schmidt et al., 2017). Herein, we selected a gravity core (CCYY1) in the North Branch of the Yangtze River and investigated its microplastic and sedimentary sequence. The aim of the study was to determine the depositional characteristics of microplastics, major factors affecting the vertical distribution of microplastics, and mechanisms through which microplastic deposition responds to extreme flood events in the Yangtze River.

2 Materials and Methods

2.1 Sampling

Core CCYY1 (121°55'42.4" E, 31°41'57.95" N) was collected from a tidal flat in the North Branch of Yangtze Estuary, Yuantuo Point, using a gravity corer and polyvinyl chloride (PVC) tube in the summer of 2019 (Figure S1 and Text S1). The 103-cm long core (174 cm if considering compaction rate) was sectioned at 1-cm intervals and then dried at 60 °C.

2.2 Microplastic analysis

The density flotation and separation method was used to extract microplastics from the sediment. The method used in this study was modified from that reported by Thompson et al. (2004) and Nuelle et al. (2014), with a recovery rate of 91%–99%. The collected particles were analysed using a stereomicroscope (Leica, MC190, Germany) and micro-Fourier transformed infrared spectroscopy

(Thermo Fisher, USA) to determine the shape, colour, size and polymer type. Detailed description of microplastic analysis and quality control measures was provided in Text S2. Finally, 859 microplastics were identified.

Although we attempted to identify all suspected particles, some of them were lost during the transfer process, which was considered an uncertainty of the experiment. Such particles were identified through visual interpretation to determine whether they were microplastics, and the number of uncertain microplastics are shown individually in the results.

2.3 Grain-size analysis

The sediment grain size was analysed at 1-cm intervals using the Malvern Mastersizer 2000 (Malvern, UK), which has a measurement range of 0.02–2000 μm and relative error within 3% for replicated measurements. The moment method (McManus, 1988) and Folk and Ward (1957) methods were used to calculate the particle size, including the mean grain size and the content of clay (<4 μm), silt (4–63 μm), and sand (>63 μm). Three parallel samples were set in the experiment, and the average value of the parallels was considered the final result.

2.4 ^{210}Pb dating

The ^{210}Pb dating method is widely used to date the sediment age on a centennial scale (Andersen et al., 2000; Arias-Ortiz et al., 2018). The dating experiment was performed at the Nanjing Institute of Geography and Limnology, China Academy of Science. The activity of radiometric ^{210}Pb was measured by direct gamma spectrometry using Ortec HPGGe GWL series, well-type, coaxial, low background, intrinsic germanium detectors (Ortec, USA). The dating method was described in detailed in Text S3.

2.5 Statistical analysis

A Spearman correlation analysis was applied to analyse the relationships between plastic production parameters, sediment grain size, and microplastic abundance (IBM SPSS Statistics, USA). Microplastic diversity was calculated based on the Simpson’s diversity index (D) proposed by Simpson (1949). Moreover, the period of microplastic abundance was measured using Software Past 4.03 in wavelet analysis (Hammer et al., 2001). The statistical method is detailed in Text S4.

3 Results

3.1 Age depth chronology

The profile of excess ^{210}Pb is shown in Figure S2. Excess ^{210}Pb decreases in moderate volatility with increasing depth, and the determination coefficient of the logarithmic fitting is $R^2 = 0.772$. The ^{210}Pb dating determined an accumulation rate of 1.23 cm/year for CCYY1 (CIC dating model), demonstrating that the core had a chronology of 1878–2011.

3.2 Microplastic abundance and characteristics

In total, 1080 microplastics were found in the samples. The microplastic abundance in the depositional record ranged from 0 to 1734.675 n/kg (dw), and the maximum concentration appeared in the surface sediment. Microplastic abundance decreased in the downcore fluctuations, with a linear fitting of $R^2 = 0.523$ (Figure 1a). There has been a rapid increase in microplastic abundance in the strata starting in the 1950s.

The microplastics found were analysed for their shape, colour, polymer type, and size. Fibres accounted for 89% of all microplastics detected, and they dominated all the sedimentary layers. Fragments, films, and granules primarily appeared after 1964 and were more common in the upper core than the downcore (Figure 1b and Figure S3a). Transparent/white was the most prevalent colour in the core, accounting for 52% of the microplastics (Figure S3b). Up to seven colours could be found in layers at depths of 14 cm (2007), 16 cm (2002), and 64 cm (1969) (Figure 1c). In terms of polymer types, up to 28 types of microplastics were found in the samples. Rayon and polyester (PES)/polyethylene terephthalate (PET) accounted for the highest percentage of microplastics in the core (48% and 33%, respectively), followed by acrylic (4%), polypropylene (PP), and polyethylene (PE) (Figure. S3c). The vertical distribution of microplastic types revealed that the types of microplastics in the upper layer were more abundant than those in the deeper layers (Figure 1d). We estimated the microplastic polymer type diversity (D_{polymer}) and mean microplastic diversity of shape, colour, and polymer type (D_{mean}). The results showed that microplastic diversity increased gradually and was relatively high during some years (Figure S4).

According to the particle size distribution curve, the lengths of most of the microplastics were in the range of 0.2 mm (87%) (Figure S3d). In the core, the quantity of plastics of large particle size was significantly lower than that of plastics of small particle size, which is consistent with our hypothesis and previous research (Y. Wang et al., 2020; C. Zhang et al., 2019). However, the number of microplastics that were < 0.3 mm was not the highest, which may be a result of the limitation of visual selection of microplastics. The proportion of small particles first decreased downcore from 2011 to the 1950s and then increased with increasing depth until 1878 as shown in Figure 1e.

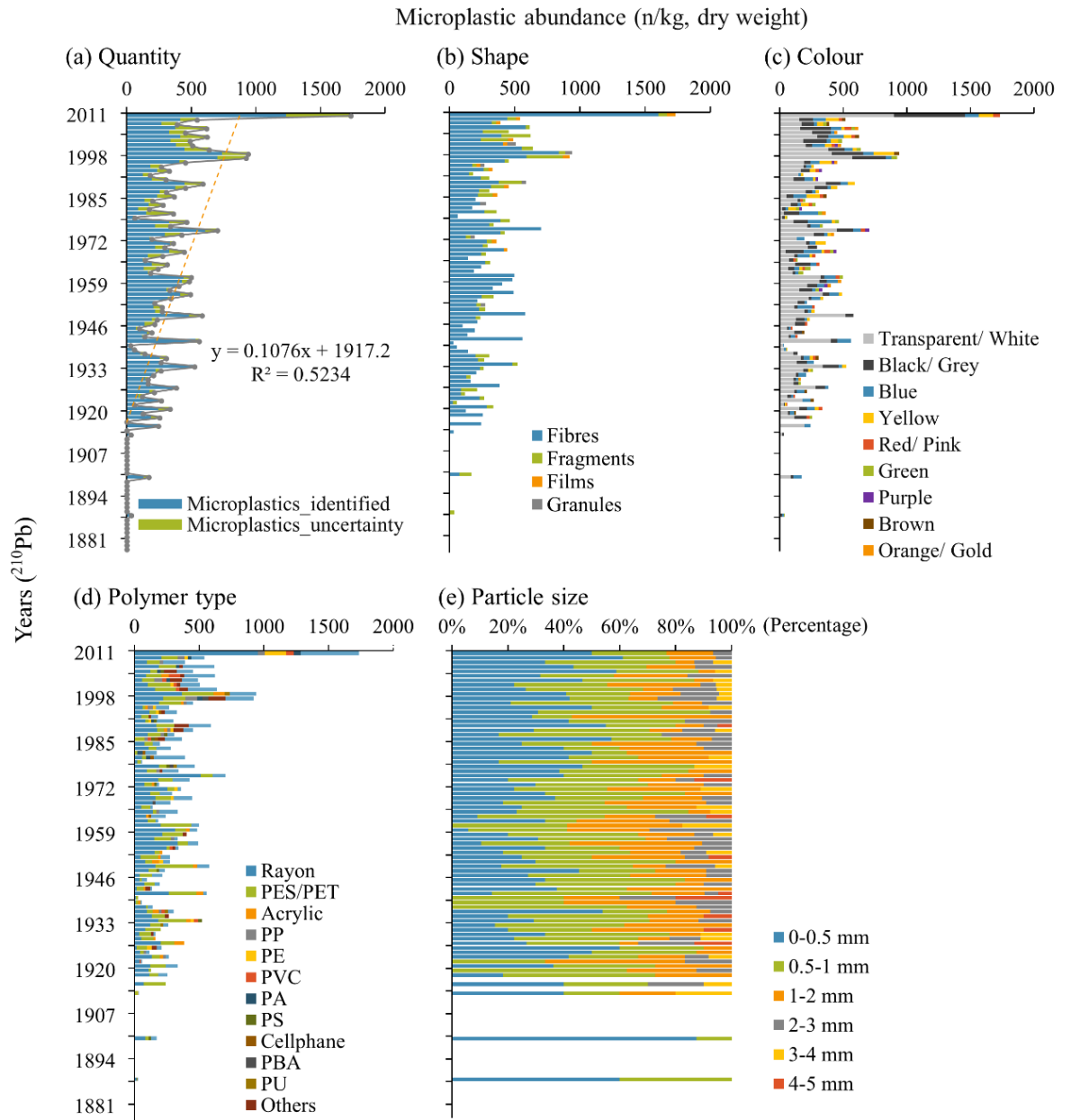


Figure 1. Vertical profile of the (a) quantity, (b) shape, (c) colour, (d) polymer type, and (e) particle size characteristics of microplastics from 1878 to 2011 in CCYY1.

3.3 Grain size characteristics of the cores

Grain size is an efficient and common index for identifying past flood events (Zhao et al., 2016). The sediment in CCYY1 was primarily silty sand and sandy silt, with a mean grain size of $96.986 \pm 20.086 \mu\text{m}$, and the clay content was low (Figure 2). The content of sand (38%–93%) and silt (7%–61%) varied in the core, whereas the clay content (0%–2%) did not change significantly. The core could be divided into three stages according to the mean grain size and sand, silt, and clay content: (1) Stage 1 (138–174 cm) represented 1878–1906. The mean grain size decreased from 118.2 μm to the minimum of the core in approximately 30 years, caused by a decrease in sand content and an increase in silt content. (2) Stage 2 (77–138 cm) referred to 1906–1956. The mean grain size fluctuated around the average grain size (107.193 μm) during this period. Two peaks with a sudden coarser grain size indicated the occurrence of extreme events. (3) Stage 3 (0–77 cm) corresponded to 1956–2019. The grain size decreased gradually and then stabilised with increasing silt content and decreasing sand content.

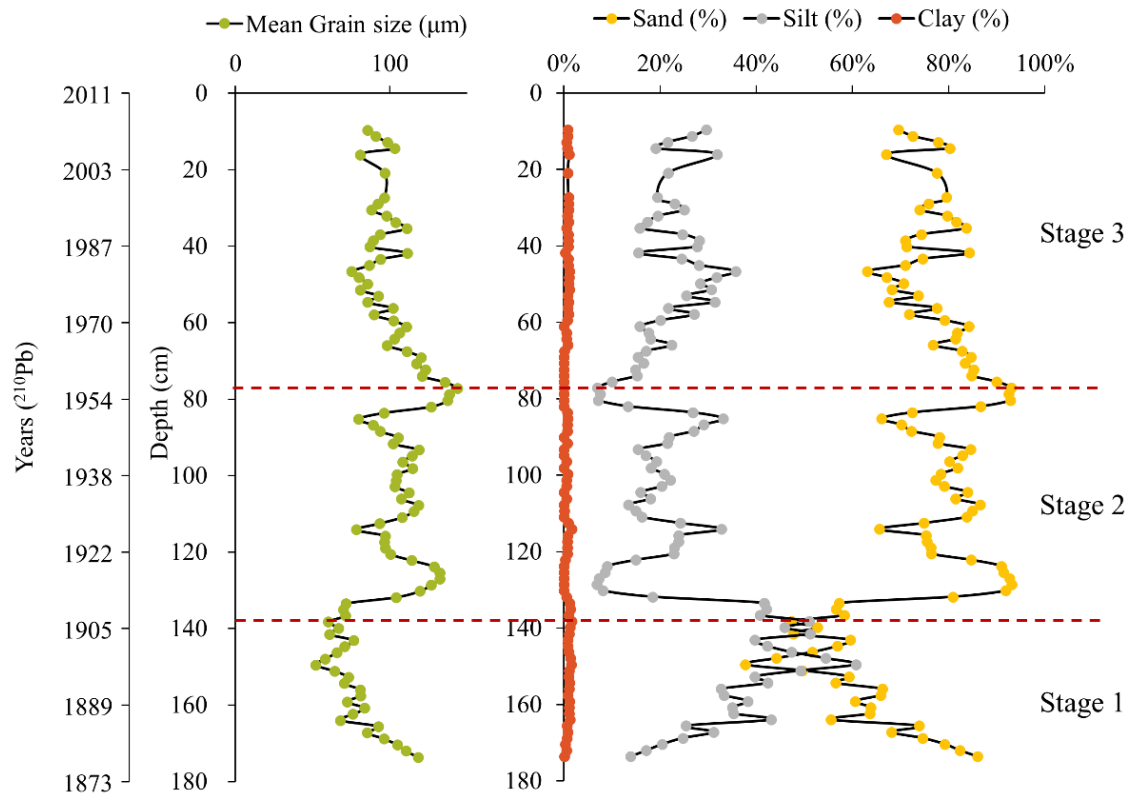


Figure 2. Grain size and sand, silt, and clay content variations in CCYY1. The dashed red line shows the diversion of the core into 3 stages according to grain size characteristics.

3.4 Result of correlation analysis and wavelet analysis

Spearman correlation analysis results showed that microplastic abundance was positively correlated with global plastic production ($R = 0.429$, $p = 0.002$, $n = 48$) and Chinese plastic production ($R = 0.420$, $p = 0.004$, $n = 45$) but was not significantly correlated with Yangtze basin plastic production ($n = 10$) (Figure 3a). Interestingly, there was a significant correlation between microplastic abundance and sediment mean grain size ($R = 0.310$, $p = 0.002$, $n = 97$). The wavelet analysis demonstrated that there were significant periodicities of 8 a and 22 a of microplastic abundance with a confidence level of 95% (Figure 3b).

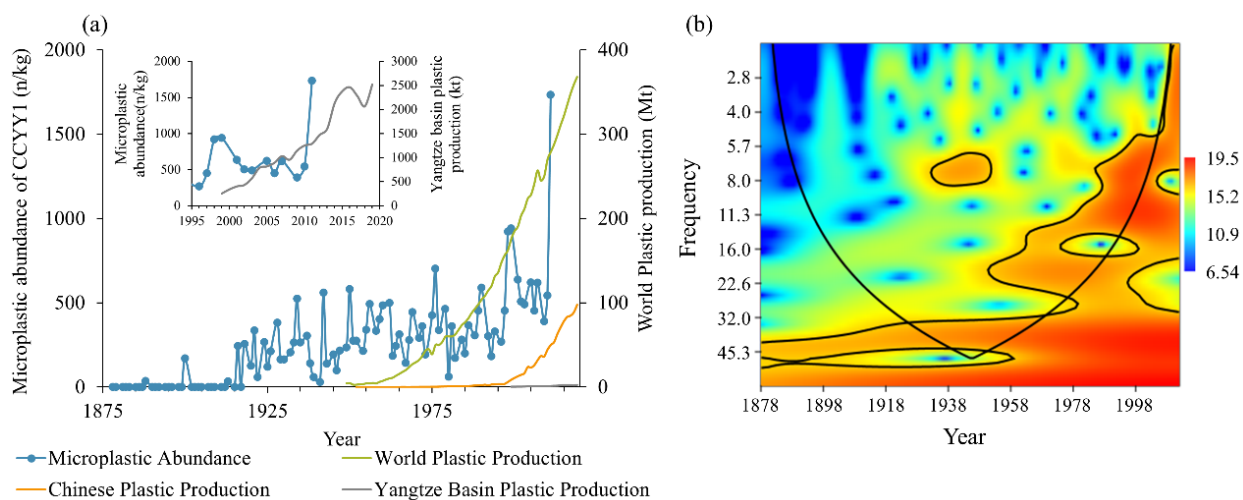


Figure 3. (a) Relationship between microplastic abundance in CCYY1 and plastic production in the world, China, and Yangtze Basin. The data source of plastic production was illustrated in Text S4. (b) Time-frequency graph of wavelet analysis for microplastic abundance in CCYY1. The colour bar on the right side demonstrates the amplitude of a particular frequency at a particular time, and high values represent substantially high amplitudes. The high amplitude value area within the solid black line implies that the significance level (p) is > 0.05 .

4 Discussion

4.1 Microplastics concentration of surface sediments compared to previous research

Microplastic abundance in different studies exhibited significant variability even when the sample sites were in the Yangtze Estuary (Table S1). The abundance of microplastics in the tidal flat was markedly higher than that in the river channel because sedimentary dynamics affect the redistribution of microplastics (Zhu et al., 2018). In the Yangtze Estuary, the river channel is in an erosional state with high velocity, whereas the tidal flat is in a depositional state with low velocity (Gao et al., 2017; Y. Zhao et al., 2015). Therefore, the variation in microplastic concentrations in the same area with different dynamics should be

considered in a comparison or discussion.

4.2 Factors affecting concentration and vertical distribution of microplastics

The change of microplastic abundance in the sedimentary record showed a synchronic trend with plastic production. The positive correlation between microplastic abundance in CCYY1 and plastic production of the world and China suggests that microplastic vertical distribution was affected by plastic production. No significant correlation was observed between microplastics and Yangtze basin plastic production, which may be due to the small sample capacity ($n=10$). Furthermore, the relationship between microplastic abundance in cores and plastic production has been reported in other well-deposited cores (Brandon et al., 2019; Dong et al., 2020). Microplastic abundance and sediment mean grain size had no direct causal relationship, although there was a significantly positive correlation between them, indicating that they may be affected by common factors, such as floods. Sediment grain size contains considerable sedimentary environmental information, and suddenly coarsened sediment may indicate high-energy events, including floods, storms, and tsunamis (Kochel & Baker, 1982; Kortekaas & Dawson, 2007). Among these disasters, floods are one of the most widespread natural disasters in the Yangtze Estuary and are frequently preserved in the sedimentary records (M. Wang et al., 2011; Wei et al., 2021); accordingly, we primarily considered the influence of floods in this study.

Notably, microplastics were found deep in the core, even at the layer of ^{210}Pb dating before the 1930s. This phenomenon has also been observed in Beibu Bay, China (Xue et al., 2020) and Santa Barbara Basin, America (Brandon et al., 2019). Although the first type of microplastics was invented in 1862 (Crawford & Quinn, 2016), most of the commonly used plastics were invented and commercially produced after the 1930s, including PVC, PS, PE, and PA (Zalasiewicz et al., 2016). Therefore, theoretically, no microplastics should be detected before the 1930s. Bioturbation and experimental pollution were used to explain the phenomenon of microplastics in deep layers (Brandon et al., 2019; Xue et al., 2020). However, after subtracting the experimental pollution, some microplastics were observed at the bottom of the core, which should not have been detected but could be attributed to bioturbation. Therefore, the extreme flood before 1930 was not discussed in this study.

4.3 Response of microplastics to extreme flood events

Flood events can significantly change the river deposition process of microplastics (Ralston et al., 2013), thereby affecting the vertical distribution of microplastics in the core. The vertical variation in microplastic abundance and mean grain size was used for comparison (Figure 4). The peak of microplastic abundance corresponded to the peak of mean grain size, which was consistent with the historic flood record in the Yangtze River compiled by Shi et al. (2004) and Wei et al. (2021). We identified nine flood layers with ^{210}Pb -determined ages of 1931 1934, 1941,1949, 1953 1956, 1969, 1975, 1990, 1998 1999, and 2011, which

corresponded to the extreme flood records of 1931, 1945, 1949, 1954, 1969, 1980, 1991, 1998, 1999, and 2010. The rapidly increasing runoff and flow velocity of flood events have sufficient energy to transport large amounts of terrigenous coarse particles, contributing to increased sand content and mean grain size (Zhao et al., 2016). The flood could also transport more microplastics to the estuary zone than usual. Land-based microplastics were accelerated to converge into the river and ocean system under heavy rain and severe flood, resulting in the increase in microplastic abundance in estuary and coastal areas after the flood (Gündoğdu et al., 2018; Veerasingam et al., 2015). In addition, microplastics deposited in the upstream sediments were released into the water and re-entered the transport system. Hurley et al. (2018) reported that microplastic concentration had decreased at most of the Irwell and Mersey river catchment sites and calculated that approximately 70% of the microplastic load fixed in the river bed was exported from the river channel. Ockelford et al. (2020) confirmed that river sediment changed from sink to source of microplastics during the flood period using the flume experiment. However, there were exceptions in the ^{210}Pb dating age of 1950, and the microplastic abundance was relatively high, while the mean grain size was relatively low.

The microplastic characteristics exhibited a significant difference following floods. Microplastic diversity was relatively high during the flood events in our study. In our study, the average diversity of microplastic polymer types of flood event layers (0.63) was slightly higher than that of the non-flood event layers (0.59) from 1931 to 2011. This is because the heavy rain in flood events enables a large amount of microplastics to enter the estuary and offshore zone from multipoint sources (Gündoğdu et al., 2018). Gündoğdu et al. (2018) also found that eight new types of microplastics were added to sediment post-flood and that the abundance of propylene/acrylic acid copolymer and styrene/allyl alcohol copolymer increased significantly.

The microplastic index (including microplastic abundance and diversity), together with grain size and other indicators, could reasonably identify flood events in the sedimentary record. At present, the proxy index of palaeo-flood events includes the grain size, organic matter (e.g., total organic carbon), geochemical elements (e.g., Zr/Rb), and pollen (Jones et al., 2012; Kochel & Baker, 1982; M. Wang et al., 2011). Their behaviours vary greatly between flood and non-flood periods because of the deposition of a large amount of coarse terrigenous particulate matter during flood periods. Grain size is the most sensitive and widely used indicator. However, with the declining trend of the diversion ratio of the North Branch, the abundance of coarse particles carried by runoff has been gradually reduced (You et al., 2018) and the mean grain size decreased from 1954, which does not sufficiently reflect the extreme floods of the Yangtze River in the record of grain size (Figure 4). Combined with the microplastic index, the flood events since the 1950s could be identified effectively, particularly the catastrophic floods in 1954, 1998 1999, and 2010, which caused substantial economic losses and casualties. Although the history of microplastics is short, they have the potential to be used as a supplementary indicator to reconstruct

flood events in recent history.

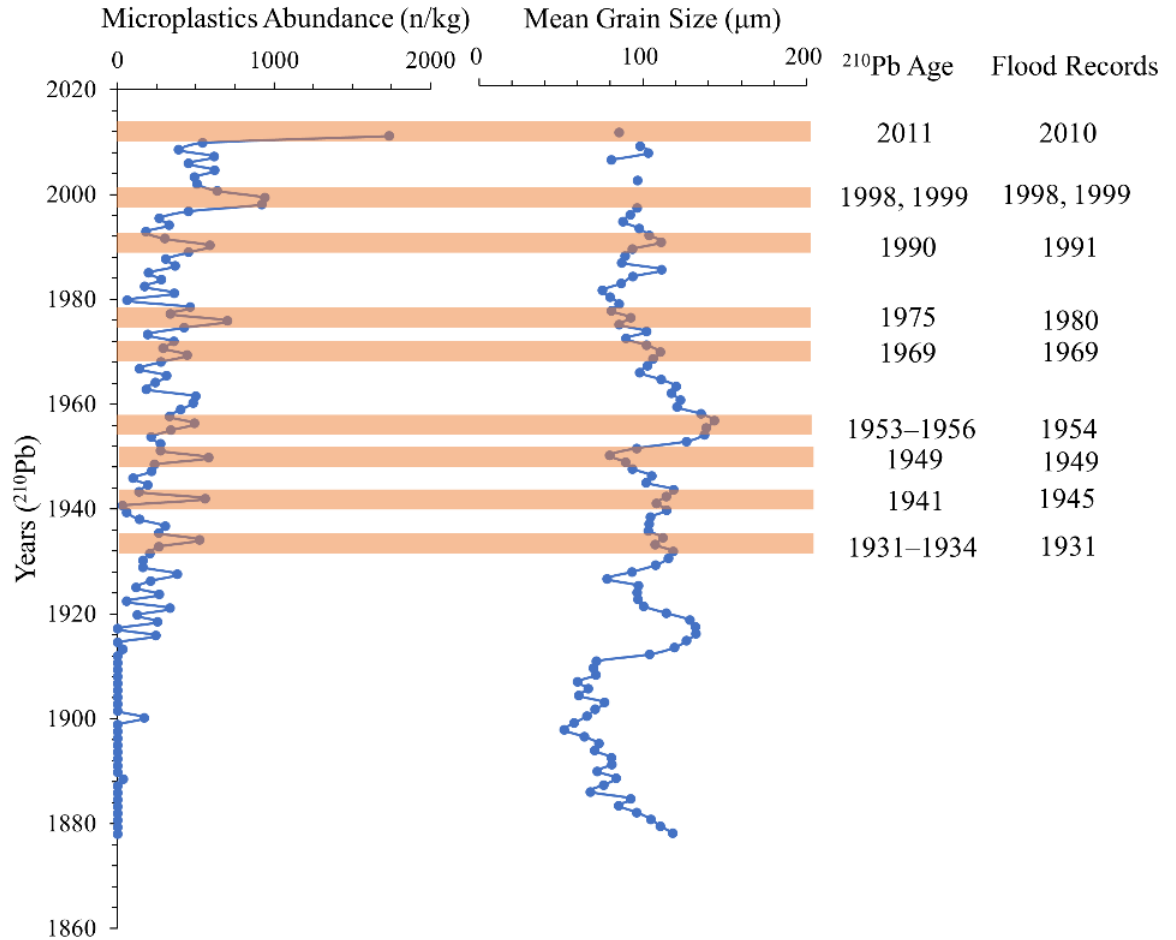


Figure 4. Extreme flood events in the middle and lower Yangtze River identified by microplastic abundance and grain size index. Extreme flood events are marked with orange blocks, corresponding ²¹⁰Pb dating age, and actual date of the floods.

4.4 Response of microplastics to the hydrology of the Yangtze River

Periodic changes in microplastic abundance and environmental elements of the Yangtze Estuary were evaluated to explore the relationship between microplastic abundance and extreme floods. The periodicities of 8 a and 22 a of microplastic abundance in CCYY1 was consistent with that of hydrological elements (e.g., streamflow and baseflow) (Qian et al., 2012; Wan et al., 2018) in the Yangtze River. In addition, periods of 8 a and 22 a have been commonly reported in studies on meteorological elements (e.g., precipitation, temperature, and evaporation) (Miao & Lin, 2003; Qian et al., 2014) and sedimentary records (e.g.,

grain size) (Zhao et al., 2016) in the Yangtze River. The two periods indicate the influence of the El Niño-Southern Oscillation (ENSO) and solar activity, respectively (Moy et al., 2002; Usoskin & Mursula, 2003).

Extreme floods are associated with river flow and precipitation in the Yangtze Estuary and are highly influenced by ENSO and solar activity (Peña et al., 2015; Q. Zhang et al., 2007). The response of floods to ENSO is a result of ENSO affecting the position and strength of the Western Pacific Subtropical High (T. Jiang et al., 2006), causing changes in precipitation and river flow and leading to an increased occurrence of floods. Some catastrophic flood events in the Yangtze Estuary, including the floods of 1936, 1954, 1983, and 1998, have been shown to be related to the occurrence of strong El Niño years (Wei et al., 2021; W. Zhang et al., 2016), resulting in a rapid increase in grain size and microplastic abundance.

5 Conclusions

We investigated the vertical distribution and characteristics of microplastics in a core of the Yangtze Estuary and explored their relationships with plastic production and extreme floods. In addition, the relationship between microplastics and floods was further elaborated from the perspective of flood records and periods. The main conclusions are as follows:

1. Microplastic abundance and polymer types exhibited increasing fluctuations over time in CCYY1 (Yuantuo Point) in the Yangtze Estuary.
2. The distribution of the core is primarily affected by plastic production and extreme floods. Microplastic abundance was significantly positively correlated with global and Chinese plastic production as well as grain size of sediments. Large amounts of terrigenous microplastics, resuspended microplastics, and coarse sediment in river channels were transported to the estuary zone during flood events, leading to a synchronous increase in microplastic abundance and mean grain size of sediments.
3. The peak values of microplastic abundance, microplastic diversity, and mean grain size of sediment were consistent with flood records in the middle and lower reaches of the Yangtze River, particularly in the catastrophic floods of the whole basin in 1931, 1954, and 1998-1999. This indicates that microplastics can be developed as a proxy index for palaeo-flood events. The periods of 8 a and 22 a were significantly detected while analysing the microplastic abundance, hydrology, and meteorology of the Yangtze River, which was related to ENSO and solar activity.

Acknowledgments

This study was supported by Geological Survey Program of the China Geological Survey (DD20190043), Natural Resources Development Special Fund of Jiangsu Province [JSZRHYKJ202001], and Central Financial Funds: Research on the dynamic monitoring network of fishery resources in the East China Sea and the improvement of marine fishing gear management system.

Data Availability Statement

The data used in our study was archived in an appropriate repository, which is available at https://zenodo.org/record/5168122#.YQ335T_iuUk.

References

- Amélineau, F., Bonnet, D., Heitz, O., Mortreux, V., Harding, A. M. A., Karnovsky, N., et al. (2016). Microplastic pollution in the Greenland Sea: Background levels and selective contamination of planktivorous diving seabirds. *Environmental Pollution*, *219*, 1131-1139. <https://doi.org/10.1016/j.envpol.2016.09.017>
- Andersen, T. J., Mikkelsen, O. A., Moller, A. L., & Morten, P. (2000). Deposition and mixing depths on some European intertidal mudflats based on ^{210}Pb and ^{137}Cs activities. *Continental Shelf Research*, *20*(12-13), 1569-1591. [https://doi.org/10.1016/S0278-4343\(00\)00038-8](https://doi.org/10.1016/S0278-4343(00)00038-8)
- Arias-Ortiz, A., Pere, M., Garcia-Orellana, J., Serrano, O., & Inés, M. (2018). Reviews and syntheses: ^{210}Pb -derived sediment and carbon accumulation rates in vegetated coastal ecosystems – setting the record straight. *Biogeosciences Discussions*, *15*, 6791-6818. <https://doi.org/10.5194/bg-15-6791-2018>
- Arthur, C., Baker, J. E., & Bamford, H. A. (2009). *Proceedings of the International Research Workshop on the Occurrence, Effects, and Fate of Microplastic Marine Debris*. Tacoma, WA: University of Washington Tacoma. Retrieved from <https://repository.library.noaa.gov/view/noaa/2509>
- Besseling, E., Quik, J. T. K., Sun, M., & Koelmans, A. A. (2017). Fate of nano- and microplastic in freshwater systems: A modeling study. *Environmental Pollution*, *220*, 540-548. <https://doi.org/10.1016/j.envpol.2016.10.001>
- Brandon, J., Jones, W., & Ohman, M. (2019). Multidecadal increase in plastic particles in coastal ocean sediments. *Science Advances*, *5*, eaax0587. <https://doi.org/10.1126/sciadv.aax0587>
- Chapman, P. M., & Wang, F. (2001). Assessing sediment contamination in estuaries. *Environmental Toxicology and Chemistry: An International Journal*, *20*(1), 3-22. <https://doi.org/10.1002/etc.5620200102>
- Chen, M., Du, M., Jin, A., Chen, S., Dasgupta, S., Li, J., et al. (2020). Forty-year pollution history of microplastics in the largest marginal sea of the western Pacific. *Geochemical Perspectives Letters*, *13*, 42-47. <https://doi.org/10.7185/geochemlet.2012>
- Cózar, A., Echevarría, F., González-Gordillo, J. I., Irigoien, X., Úbeda, B., Hernández-León, S., et al. (2014). Plastic debris in the open ocean. *Proceedings of the National Academy of Sciences*, *111*(28), 10239. <http://www.pnas.org/content/111/28/10239.abstract>
- Crawford, C. B., & Quinn, B. (2016). *Microplastic Pollutants*. Elsevier Limited.

- Dahl, M., Bergman, S., Björk, M., Diaz-Almela, E., Granberg, M., Gullström, M., et al. (2021). A temporal record of microplastic pollution in Mediterranean seagrass soils. *Environmental Pollution*, *273*, 116451. <https://doi.org/10.1016/j.envpol.2021.116451>
- Dai, Z., Mei, X., Darby, S. E., Lou, Y., & Li, W. (2018). Fluvial sediment transfer in the Changjiang (Yangtze) river-estuary depositional system. *Journal of Hydrology*, *566*, 719-734. <https://doi.org/10.1016/j.jhydrol.2018.09.019>
- Ding, Y., Zou, X., Wang, C., Feng, Z., Wang, Y., Fan, Q., & Chen, H. (2021). The abundance and characteristics of atmospheric microplastic deposition in the northwestern South China Sea in the fall. *Atmospheric Environment*, *253*, 118389. <https://doi.org/10.1016/j.atmosenv.2021.118389>
- Dong, M., Luo, Z., Jiang, Q., Xing, X., Zhang, Q., & Sun, Y. (2020). The rapid increases in microplastics in urban lake sediments. *Scientific Reports*, *10*(1), 848. <https://doi.org/10.1038/s41598-020-57933-8>
- Folk, R. L., & Ward, W. C. (1957). Brazos River bar [Texas]; a study in the significance of grain size parameters. *Journal of Sedimentary Research*, *27*(1), 3-26. <https://doi.org/10.1306/74D70646-2B21-11D7-8648000102C1865D>
- Gao, J. H., Jia, J., Sheng, H., Yu, R., Li, G. C., Wang, Y. P., et al. (2017). Variations in the transport, distribution, and budget of ²¹⁰Pb in sediment over the estuarine and inner shelf areas of the East China Sea due to Changjiang catchment changes. *Journal of Geophysical Research: Earth Surface*, *122*(1), 235-247. <https://doi.org/10.1002/2016JF004130>
- Gray, A. D., Wertz, H., Leads, R. R., & Weinstein, J. E. (2018). Microplastic in two South Carolina Estuaries: Occurrence, distribution, and composition. *Marine Pollution Bulletin*, *128*, 223-233. <https://doi.org/10.1016/j.marpolbul.2018.01.030>
- Gündoğdu, S., Çevik, C., Ayat, B., Aydoğan, B., & Karaca, S. (2018). How microplastics quantities increase with flood events? An example from Mersin Bay NE Levantine coast of Turkey. *Environmental Pollution*, *239*, 342-350. <https://doi.org/10.1016/j.envpol.2018.04.042>
- Hammer, Ø., Harper, D. A. T., & Ryan, P. D. (2001). Past: Paleontological statistics software package for education and data analysis. *Palaeontologia Electronica*, *4*(1), 1-9. http://palaeo-electronica.org/2001_1/past/issue1_01.htm
- Hurley, R., Woodward, J., & Rothwell, J. J. (2018). Microplastic contamination of river beds significantly reduced by catchment-wide flooding. *Nature Geoscience*, *11*(4), 251-257. <https://doi.org/10.1038/s41561-018-0080-1>
- Jambeck, J. R., Geyer, R., Wilcox, C., Siegler, T. R., Perryman, M., Andrady, A., et al. (2015). Plastic waste inputs from land into the ocean. *Science*, *347*(6223), 768-771. <https://doi.org/10.1126/science.1260352>
- Jiang, T., Zhang, Q., Zhu, D., & Wu, Y. (2006). Yangtze floods and droughts (China) and teleconnections with ENSO activities (1470–2003). *Quaternary*

- International*, 144(1), 29-37. <https://doi.org/10.1016/j.quaint.2005.05.010>
- Jiang, Y., & Jiang, M. (2013). Plastics: The Discovery in the World and Development in China. *Advanced Materials Research*, 750, 811-815. <https://doi.org/10.4028/www.scientific.net/amr.750-752.811>
- Jones, A. F., Macklin, M. G., & Brewer, P. A. (2012). A geochemical record of flooding on the upper River Severn, UK, during the last 3750 years. *Geomorphology*, 179, 89-105. <https://doi.org/10.1016/j.geomorph.2012.08.003>
- Katija, K., Choy, C. A., Sherlock, R. E., Sherman, A. D., & Robison, B. H. (2017). From the surface to the seafloor: How giant larvaceans transport microplastics into the deep sea. *Science Advances*, 3(8), e1700715. <https://doi.org/10.1126/sciadv.1700715>
- Kochel, R. C., & Baker, V. R. (1982). Paleoflood hydrology. *Science*, 215(4531), 353-361. <https://doi.org/10.1126/science.215.4531.353>
- Kortekaas, S., & Dawson, A. G. (2007). Distinguishing tsunami and storm deposits: an example from Martinhal, SW Portugal. *Sedimentary Geology*, 200(3-4), 208-221. <https://doi.org/10.1016/j.sedgeo.2007.01.004>
- Laxague, N. J. M., Özgökmen, T. M., Haus, B. K., Novelli, G., Shcherbina, A., Sutherland, P., et al. (2018). Observations of near-surface current shear help describe oceanic oil and plastic transport. *Geophysical Research Letters*, 45(1), 245-249. <https://doi.org/10.1002/2017GL075891>
- Lebreton, L., & Andrady, A. (2019). Future scenarios of global plastic waste generation and disposal. *Palgrave Communications*, 5(1), 6. <https://doi.org/10.1057/s41599-018-0212-7>
- Lebreton, L., van der Zwet, J., Damsteeg, J.-W., Slat, B., Andrady, A., & Reisser, J. (2017). River plastic emissions to the world's oceans. *Nature Communications*, 8(1), 15611. <https://doi.org/10.1038/ncomms15611>
- Lobelle, D., & Michael, C. (2011). Early microbial biofilm formation on marine plastic debris. *Marine Pollution Bulletin*, 62(1), 197-200. <https://doi.org/10.1016/j.marpolbul.2010.10.013>
- Long, M., Moriceau, B., Gallinari, M., Lambert, C., Huvet, A., Raffray, J., & Soudant, P. (2015). Interactions between microplastics and phytoplankton aggregates: Impact on their respective fates. *Marine Chemistry*, 175, 39-46. <https://doi.org/10.1016/j.marchem.2015.04.003>
- Mai, L., Sun, X. F., Xia, L. L., Bao, L. J., Liu, L. Y., & Zeng, E. Y. (2020). Global Riverine Plastic Outflows. *Environmental Science and Technology*, 54(16), 10049-10056. <https://doi.org/10.1021/acs.est.0c02273>
- Martin, C., Baalkhuyur, F., Valluzzi, L., Saderne, V., Cusack, M., Almahsheer, H., et al. (2020). Exponential increase of plastic burial in mangrove sediments as a major plastic sink. *Science Advances*, 6(44), eaaz5593. <https://doi.org/10.1126/sciadv.aaz5593>

- McManus, J. (1988). Grain size determination and interpretation. *Techniques, in Sedimentology*, 63-85. <https://ci.nii.ac.jp/naid/10003977077/en/>
- Miao, J., & Lin, Z. (2003). Study on the characteristics of the precipitation of nine regions in China and their physical causes. *Journal of Tropical Meteorology*, 19(4), 377-388. <https://doi.org/10.3969/j.issn.1004-4965.2003.04.005>
- Moy, C. M., Seltzer, G. O., Rodbell, D. T., & Anderson, D. M. (2002). Variability of El Niño/Southern Oscillation activity at millennial timescales during the Holocene epoch. *Nature*, 420(6912), 162-165. <https://doi.org/10.1038/nature01194>
- Nuelle, M.-T., Dekiff, J. H., Remy, D., & Fries, E. (2014). A new analytical approach for monitoring microplastics in marine sediments. *Environmental Pollution*, 184, 161-169. <https://doi.org/10.1016/j.envpol.2013.07.027>
- Ockelford, A., Cundy, A., & Ebdon, J. E. (2020). Storm Response of Fluvial Sedimentary Microplastics. *Scientific Reports*, 10(1), 1865. <https://doi.org/10.1038/s41598-020-58765-2>
- Peña, J. C., Schulte, L., Badoux, A., Barriendos, M., & Barrera-Escoda, A. (2015). Influence of solar forcing, climate variability and modes of low-frequency atmospheric variability on summer floods in Switzerland. *Hydrology and Earth System Sciences*, 19(9), 3807-3827. <https://doi.org/10.5194/hess-19-3807-2015>
- Plastics- the facts 2020 -An analysis of European plastics production, demand and waste data.* Brussels: Plastic Europe (2020). Retrieved from https://www.plasticseurope.org/application/files/3416/2270/7211/Plastics_the_facts-WEB-2020_versionJun21_final.pdf
- Qian, K., Wan, L., Wang, X., Lv, J., & Liang, S. (2012). Periodical characteristics of baseflow in the source region of the Yangtze River. *Journal of Arid Land*, 4(2), 113-122. <https://doi.org/10.3724/SP.J.1227.2012.00113>
- Qian, K., Wang, X., Lv, J., & Wan, L. (2014). The wavelet correlative analysis of climatic impacts on runoff in the source region of Yangtze River, in China. *International Journal of Climatology*, 34(6), 2019-2032. <https://doi.org/10.1002/joc.3818>
- Ralston, D. K., Warner, J. C., Geyer, W. R., & Wall, G. R. (2013). Sediment transport due to extreme events: The Hudson River estuary after tropical storms Irene and Lee. *Geophysical Research Letters*, 40(20), 5451-5455. <https://doi.org/10.1002/2013GL057906>
- Ridgway, J., & Shimmield, G. (2002). Estuaries as repositories of historical contamination and their impact on shelf seas. *Estuarine, Coastal and Shelf Science*, 55(6), 903-928. <https://doi.org/10.1006/ecss.2002.1035>
- Schmidt, C., Krauth, T., & Wagner, S. (2017). Export of Plastic Debris by Rivers into the Sea. *Environmental Science and Technology*, 51(21), 12246-12253. <https://doi.org/10.1021/acs.est.7b02368>

- Shi, Y. F., Jiang, T., Su, B., Chen, J. Q., & Qin, N. X. (2004). Preliminary analysis on the relation between the evolution of heavy flood in the Yangtze River catchment and the climate changes since 1840. *Journal of lake sciences*, *16*(4), 289-297. <https://doi.org/10.18307/2004.0401>
- Simpson, E. H. (1949). Measurement of Diversity. *Nature*, *163*(4148), 688-688. <https://doi.org/10.1038/163688a0>
- Sun, J., Wang, M.-H., & Ho, Y.-S. (2012). A historical review and bibliometric analysis of research on estuary pollution. *Marine Pollution Bulletin*, *64*(1), 13-21. <https://doi.org/10.1016/j.marpolbul.2011.10.034>
- Thompson, R. C., Olson, Y., Mitchell, R. P., Davis, A., Rowland, S. J., John, A. W. G., et al. (2004). Lost at Sea: Where Is All the Plastic? *Science*, *304*(5672), 838. <https://doi.org/10.1126/science.1094559>
- Usoskin, I. G., & Mursula, K. (2003). Long-Term Solar Cycle Evolution: Review of Recent Developments. *Solar Physics*, *218*(1), 319-343. <https://doi.org/10.1023/B:SOLA.0000013049.27106.07>
- Veerasingam, S., Mugilarasan, M., Venkatachalapathy, R., & Vethamony, P. (2015). Influence of 2015 flood on the distribution and occurrence of microplastic pellets along the Chennai coast, India. *Marine Pollution Bulletin*, *109*, 196-204. <https://doi.org/10.1016/j.marpolbul.2016.05.082>
- Veerasingam, S., Saha, M., Suneel, V., Vethamony, P., Rodrigues, A. C., Bhat-tacharyya, S., & Naik, B. G. (2016). Characteristics, seasonal distribution and surface degradation features of microplastic pellets along the Goa coast, India. *Chemosphere*, *159*, 496-505. <https://doi.org/10.1016/j.chemosphere.2016.06.056>
- Wan, Z. W., Lian, L. C., Jia, Y. L., Hong, W. J., & Jiang, M. X. (2018). Trend phases and periodic changes of discharges from Yangtze River in past 150 years. *Bulletin of Soil and Water Conservation*, *38*(2), 14-18. <https://doi.org/10.13961/j.cnki.stbctb.2018.02.003>
- Wang, C., Zhao, J., & Xing, B. (2021). Environmental source, fate, and toxicity of microplastics. *Journal of Hazardous Materials*, *407*, 124357. Review. <https://doi.org/10.1016/j.jhazmat.2020.124357>
- Wang, M., Zheng, H., Xie, X., Fan, D., Yang, S., Zhao, Q., & Wang, K. (2011). A 600-year flood history in the Yangtze River drainage: comparison between a subaqueous delta and historical records. *Chinese Science Bulletin*, *56*(2), 188-195. <https://doi.org/10.1007/s11434-010-4212-2>
- Wang, Y., Zou, X., Peng, C., Qiao, S., Wang, T., Yu, W., et al. (2020). Occurrence and distribution of microplastics in surface sediments from the Gulf of Thailand. *Marine Pollution Bulletin*, *152*, 110916. <https://doi.org/10.1016/j.marpolbul.2020.110916>
- Wei, L., Fan, D., Wu, Y., & Ren, F. (2021). High resolution flood records in the

- Yangtze subaqueous delta during the past century and control mechanism. *Geological Bulletin of China*, 40(5), 707-720. http://dzhtb.cgs.cn/gbc/ch/reader/view_abstract.aspx?file_no=2021050501
- Wright, S. L., Thompson, R. C., & Galloway, T. S. (2013). The physical impacts of microplastics on marine organisms: a review. *Environmental Pollution* 178, 483-492. Review. <https://doi.org/10.1016/j.envpol.2013.02.031>
- Xue, B., Zhang, L., Li, R., Wang, Y., Guo, J., Yu, K., & Wang, S. (2020). Underestimated Microplastic Pollution Derived from Fishery Activities and "Hidden" in Deep Sediment. *Environmental Science and Technology*, 54(4), 2210-2217. <https://doi.org/10.1021/acs.est.9b04850>
- You, B. W., Zhang, G. A., Li, Y. M., & Li, Z. H. (2018). Sediment Characteristics and Transport Trend in North Branch and Offshore Area of Yangtze Estuary in the Last 30 Years. *Resources and Environment in the Yangtze Basin*, 27(10), 2328-2338.
- Zalasiewicz, J., Waters, C. N., Sul, J. I. D., Corcoran, P. L., & Yamin, Y. (2016). The geological cycle of plastics and their use as a stratigraphic indicator of the Anthropocene. *Anthropocene*, 13, 4-17. <https://doi.org/10.1016/j.ancene.2016.01.002>
- Zhang, C., Zhou, H., Cui, Y., Wang, C., Li, Y., & Zhang, D. (2019). Microplastics in offshore sediment in the yellow Sea and east China Sea, China. *Environmental Pollution*, 244, 827-833. <https://doi.org/10.1016/j.envpol.2018.10.102>
- Zhang, Q., Xu, C.-Y., Jiang, T., & Wu, Y. (2007). Possible influence of ENSO on annual maximum streamflow of the Yangtze River, China. *Journal of Hydrology*, 333(2-4), 265-274. <https://doi.org/10.1016/j.jhydrol.2006.08.010>
- Zhang, W., Jin, F. F., Stuecker, M. F., Wittenberg, A. T., Timmermann, A., Ren, H. L., et al. (2016). Unraveling El Niño's impact on the East Asian monsoon and Yangtze River summer flooding. *Geophysical Research Letters*, 43(21), 11-375. <https://doi.org/10.1002/2016GL071190>
- Zhao, S., Zhu, L., & Li, D. (2015). Microplastic in three urban estuaries, China. *Environmental Pollution*, 206, 597-604. <https://doi.org/10.1016/j.envpol.2015.08.027>
- Zhao, Y., Zou, X., Gao, J., & Wang, C. (2016). Recent sedimentary record of storms and floods within the estuarine-inner shelf region of the East China Sea. *Holocene*, 27(3), 439-449. <https://doi.org/10.1177/0959683616660165>
- Zhao, Y., Zou, X., Gao, J., Xu, X., Wang, C., Tang, D., et al. (2015). Quantifying the anthropogenic and climatic contributions to changes in water discharge and sediment load into the sea: A case study of the Yangtze River, China. *Science of The Total Environment*, 536, 803-812. <https://doi.org/10.1016/j.scitotenv.2015.07.119>
- Zhu, X. T., Yi, J., Qiang, L. Y., & Cheng, J. P. (2018). Distribution and Settlement of Microplastics in the Surface Sediment of Yangtze Estuary. *Huanjing*

Kexue/Environmental Science, 39(5), 2067-2074. <https://doi.org/10.13227/j.hjks.201709032>

Figure 1. Vertical profile of the (a) quantity, (b) shape, (c) colour, (d) polymer type, and (e) particle size characteristics of microplastics from 1878 to 2011 in CCYY1.

Figure 2. Grain size and sand, silt, and clay content variations in CCYY1. The dashed red line shows the diversion of the core into 3 stages according to grain size characteristics.

Figure 3. (a) Relationship between microplastic abundance in CCYY1 and plastic production in the world, China, and Yangtze Basin. The data source of plastic production was illustrated in Text S4. (b) Time-frequency graph of wavelet analysis for microplastic abundance in CCYY1. The colour bar on the right side demonstrates the amplitude of a particular frequency at a particular time, and high values represent substantially high amplitudes. The high amplitude value area within the solid black line implies that the significance level (p) is > 0.05 .

Figure 4. Extreme flood events in the middle and lower Yangtze River identified by microplastic abundance and grain size index. Extreme flood events are marked with orange blocks, corresponding ^{210}Pb dating age, and actual date of the floods.